

MODIS Thermal Emissive Bands Calibration Algorithm and On-orbit Performance

X. (Jack) Xiong^{*a}, K. Chiang^a, B. Guenther^b, and W. Barnes^c

^aScience Systems and Applications, Inc., 10210 Greenbelt Road, Suite 600, Lanham, MD 20706;

^bLockheed Martin Corporation, 8455 Colesville Road, Suite 960, Silver Spring, MD 20910;

^cLaboratory for Hydrospheric Processes, NASA/GSFC, Greenbelt, MD 20771

ABSTRACT

The MODerate Resolution Imaging Spectroradiometer (MODIS) is one of the key instruments for the NASA's Earth Observing System (EOS). MODIS ProtoFlight Model (PFM) was launched on-board the EOS Terra spacecraft on December 18, 1999 and the MODIS Flight Model (FM-1) was launched on-board the EOS Aqua spacecraft on May 4, 2002. MODIS has 36 spectral bands with wavelengths ranging from 0.41 to 14.5 μ m and nadir spatial resolutions of 250m (2 bands), 500m (5 bands), and 1km (29 bands). The sensor's 20 reflective solar bands (RSB) from 0.41 to 2.1 μ m are calibrated on-orbit by a solar diffuser (SD) and a solar diffuser stability monitor (SDSM). The other 16 thermal emissive bands (TEB) with wavelengths above 3.7 μ m are calibrated by a blackbody. This paper follows the discussions on the RSB calibration and instrument performance presented in a separate paper (Xiong *et. al.*) in these proceedings, and focuses on the 16 thermal emissive bands (TEB).

Keywords: Terra, Aqua, MODIS, calibration, thermal emissive bands, blackbody

1. INTRODUCTION

Following our discussions on the MODIS reflective solar bands (RSB) calibration algorithm and on-orbit performance¹ in a paper also in these proceedings, we focus on the MODIS thermal emissive bands (TEB) with wavelengths above 3.7 μ m. Readers are referred to the RSB paper and other references for a general review of the NASA EOS Terra and Aqua MODIS instruments and the many applications that are developed from using MODIS global data sets²⁻⁴. Terra MODIS (PFM) has been providing the science community and public users global data sets for the study of the land, oceans, and atmosphere for more than two and a half years in a near Sun-synchronous polar orbit of 10:30AM equator crossing time. With the recent launch of Aqua spacecraft (1:30 PM orbit), this coverage is enhanced such that the same Earth scene can be viewed both in the morning and in the afternoon. The MODIS L1B algorithm converts instrument response to the radiometrically calibrated data products (reflectance factor for the RSB, radiance for the TEB). In this paper, we discuss the TEB on-orbit calibration algorithm, its implementation strategy in the Level 1B code (L1B), and instrument on-orbit performance for the thermal emissive bands, including the differences between the Terra MODIS and Aqua MODIS.

2. THERMAL EMISSIVE BANDS AND INSTRUMENT BACKGROUND

There are 16 thermal emissive bands, covering the middle wave infrared (MWIR: bands 20-25) and long wave infrared (LWIR: bands 27-36) spectral regions. Table 1 summarizes the TEB key specification, including the spectral band center wavelength, typical scene radiance, and the corresponding noise equivalent temperature difference (NE Δ T). All thermal emissive bands are located on two cold focal plane assemblies (CFPAs): a short wave and middle wave infrared (SMIR) FPA and a long wave infrared (LWIR) FPA. The CFPAs are nominally controlled on-orbit at 83K using a passive radiative cooler. An on-board calibrator blackbody (BB) is used for the TEB calibration. The blackbody temperature can be varied from instrument ambient (about 270K) to 315K. Normally, it is set at 290K for Terra MODIS and 285K for Aqua MODIS. The temperature of the BB is measured by 12 thermistors embedded in the BB and is traceable to the NIST temperature scale.

Band	CW (μm)	T_Ltyp (K)	NEdT (K) (spec)	NEdT (K) Terra (A-I)	NEdT (K) Terra (B)	NEdT (K) Terra (A-II)	NEdT (K) Aqua (B)
20	3.75	300	0.05	0.03	0.03	0.02	0.02
21	3.96	335	0.20	0.15	0.16	0.14	0.21
22	3.96	300	0.07	0.02	0.03	0.03	0.02
23	4.05	300	0.07	0.02	0.02	0.02	0.02
24	4.47	250	0.25	0.13	0.13	0.13	0.11
25	4.52	275	0.25	0.05	0.05	0.05	0.04
27	6.72	240	0.25	0.10	0.11	0.09	0.10
28	7.33	250	0.25	0.05	0.05	0.05	0.05
29	8.55	300	0.05	0.02	0.03	0.02	0.02
30	9.73	250	0.25	0.11	0.15	0.10	0.07
31	11.03	300	0.05	0.03	0.03	0.02	0.02
32	12.02	300	0.05	0.04	0.04	0.04	0.03
33	13.34	260	0.25	0.13	0.13	0.12	0.08
34	13.64	250	0.25	0.23	0.25	0.26	0.12
35	13.94	240	0.25	0.23	0.22	0.22	0.15
36	14.24	220	0.35	0.43	0.43	0.43	0.23

Table 1: MODIS thermal emissive bands (TEB) key specifications. On-orbit NEdT of Terra MODIS in three operational configurations and current NEdT of Aqua MODIS (middle detectors)

Figure 1 shows the MODIS scan cavity and its on-board calibrators (OBCs). The thermal emissive bands are calibrated on-orbit by a flat panel v-grooved blackbody (BB) on a scan by scan basis. Each scan the sensor views the blackbody (BB) and deep space through the instrument space view (SV) port for the calibration, and then the Earth view (EV) for the scene retrieval. The BB provides a known radiance source for each detector's calibration. The instrument thermal background is determined by the sensor's response during the space view.

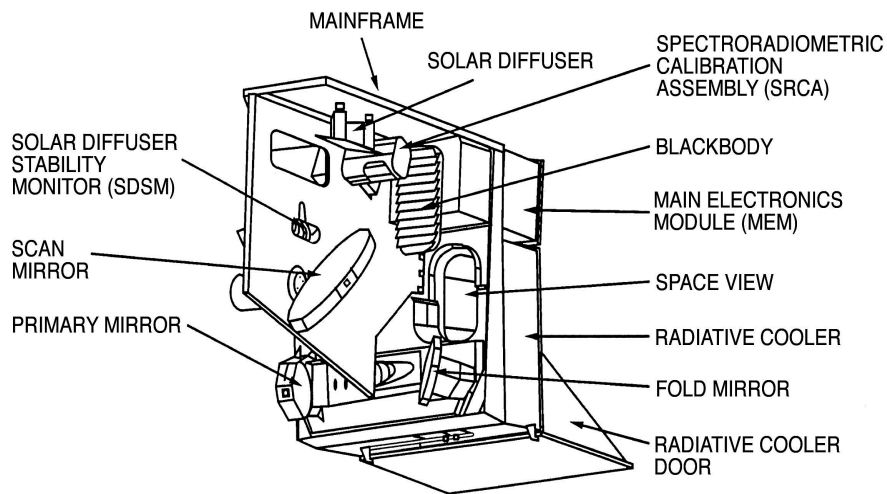


Figure 1: MODIS scan cavity and on-board calibrators: solar diffuser (SD), solar diffuser stability monitor (SDSM), blackbody (BB), and spectroradiometric calibration assembly (SRCA)

3. TEB CALIBRATION ALGORITHM

All 16 thermal emissive bands (B20-25, 27-36) are of the same spatial resolution (1km at nadir) with each having 10 detectors aligned in the along track direction. The calibration is performed for each band, detector, and mirror side. The TEB product from L1B is top of the atmosphere (TOA) radiance. When the sensor views an Earth scene via its scan mirror, the total path radiance includes the contributions from the Earth view (EV) radiance, the radiance due to the scan mirror (SM) emission, and the thermal background (BKG). Thus

$$L_{EV_Path} = RVS_{EV} \cdot L_{EV} + (1 - RVS_{EV}) \cdot L_{SM} + L_{BKG}, \quad (1)$$

where L is the spectral band averaged radiance, and RVS_{EV} is the scan mirror response versus scan angle. The term $(1 - RVS_{EV})$ is equivalent to the emissivity of the scan mirror, which varies with the scan angle or the angle of incidence (AOI) on the scan mirror. Similarly, when the sensor views deep space through the SV port, the total path radiance can be expressed as,

$$L_{SV_Path} = (1 - RVS_{SV}) \cdot L_{SM} + L_{BKG}. \quad (2)$$

It only includes the scan mirror term and the background term but has no direct source term. The scan mirror terms in Eqn. 1 and Eqn. 2 are not the same since the RVS is a function of the AOI on the scan mirror. The difference between Eqn. 1 and Eqn. 2 is related to the sensor's response difference between the EV and SV. Using a quadratic approach, the path radiance difference is written as,

$$RVS_{EV} \cdot L_{EV} + (RVS_{SV} - RVS_{EV}) \cdot L_{SM} = a_0 + b_1 \cdot dn_{EV} + a_2 \cdot dn_{EV}^2, \quad (3)$$

where dn_{EV} is the sensor's response to the Earth view in terms of the digital number (DN_{EV}) with the average response to the space view $\langle DN_{SV} \rangle$ in the same scan subtracted

$$dn_{EV} = DN_{EV} - \langle DN_{SV} \rangle. \quad (4)$$

There are 50 frames of data collected in the SV sector. A similar equation for the BB calibration can be written using the sensor's response to the blackbody (BB),

$$\begin{aligned} RVS_{BB} \cdot \epsilon_{BB} \cdot L_{BB} + (RVS_{SV} - RVS_{BB}) \cdot L_{SM} + RVS_{BB} \cdot (1 - \epsilon_{BB}) \cdot \epsilon_{CAV} \cdot L_{CAV} \\ = a_0 + b_1 \cdot dn_{BB} + a_2 \cdot dn_{BB}^2 \end{aligned} \quad (5)$$

The first term on the LHS is the source term from the BB, the second term is from the scan mirror, and the third term comes from contributions from the instrument scan cavity. The emissivity of the BB and that of the scan cavity are represented by ϵ_{BB} and ϵ_{CAV} . Note we use b_1 , instead of a_1 , in these equations to emphasize the scan by scan computation of the linear coefficient. Figure 2 illustrates the calculation of dn_{BB} for the three middle detectors of Aqua B33 on a scan by scan basis,

$$dn_{BB} = \langle DN_{BB} \rangle - \langle DN_{SV} \rangle \quad (6)$$

Because of the thermal drift of the instrument background and the DC restore of the electronics (used to maintain the response's dynamic range), dn_{BB} must be computed every scan (same mirror side) for each band and detector. dn_{BB} is related to the radiance from the blackbody, scan mirror, and instrument cavity. The radiance term, e.g. L_{SM} , is computed using Planck's equation averaged over the detector's relative spectral response (RSR),

$$L_{SM}(\lambda, T_{SM}) = \frac{\sum RSR(\lambda) \cdot Planck(\lambda, T_{SM})}{\sum RSR(\lambda)}. \quad (7)$$

The offset term a_0 and nonlinear term a_2 in Equations 3 and 5 are provided in the LUTs with values determined either from pre-launch calibration or from on-orbit BB warm-up and cool-down cycles. The BB cycle provides the TEB detectors's responses over a range of BB temperatures (thus the radiance) from 270K to 315K. The linear coefficient b_1 of each detector is determined every scan knowing the BB temperature, scan mirror and cavity temperatures, and the sensor's response to the BB view and the SV view using Eqn. 5. Other parameters, such as emissivity and RVS, determined from pre-launch calibration, are also provided in the L1B LUTs.

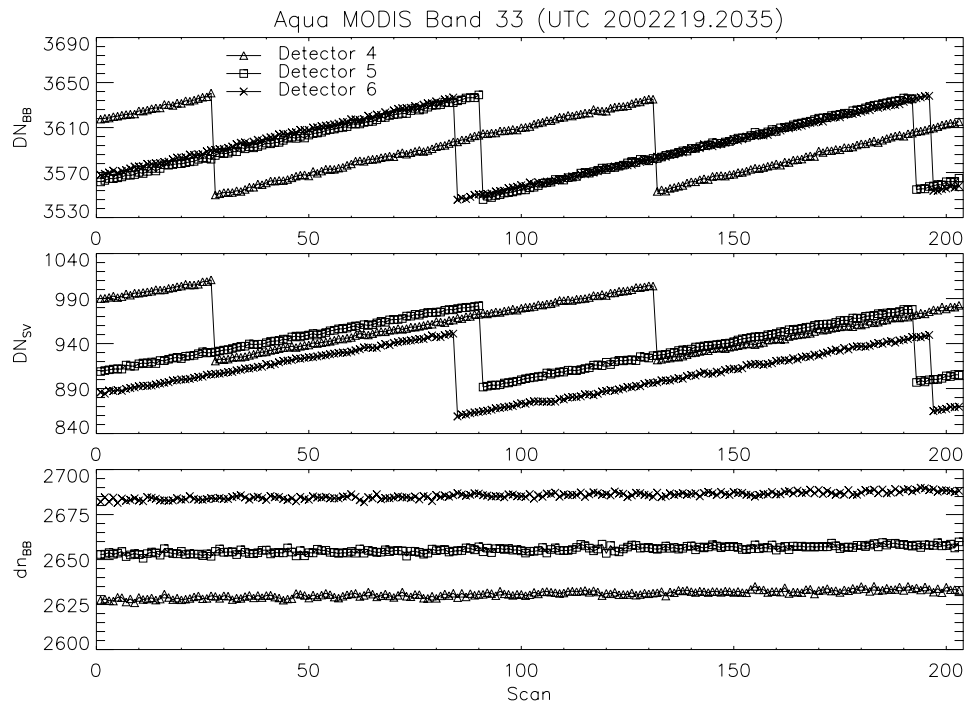


Figure 2: Aqua MODIS B33 detectors responses versus scan (detectors 4, 5, and 6). DN_{BB} and DN_{Sv} are averaged over 50 frames in each scan. The slow variation of the raw DNs is due to the instrument thermal drift, the occasional large change of the raw DNs from one scan to another is due to the electronic s DC restore

4. SPECIAL CONSIDERATIONS

Equations 1-7 in the previous section provide the MODIS thermal emissive bands calibration algorithm. In this section, we present special considerations used in the thermal emissive bands calibration. These considerations include band 21 (fire detection band) calibration strategy, the algorithm for removing Terra MODIS photo-conductive (PC) bands optical leak, and the approach used to retain the Aqua MODIS band 33, 35, and 36 on-orbit calibration when the blackbody temperature is above their saturation limits. These issues were identified from pre-launch testing and characterized prior to the instruments launches. Using on-orbit data sets, we are able to track potential changes and monitor the performance of these special algorithms or approaches.

4.1 Band 21 Calibration

MODIS band 21 consists of low gain photovoltaic (PV) detectors with a center wavelength at $3.96\mu\text{m}$ and specified typical scene temperature of 335K and a maximum of 500K. This middle-wave spectral band is used primarily for fire detection. Figures 3 and 4 illustrate all 16 thermal emissive bands on-orbit response (one detector per band) as a function of blackbody temperature, from instrument ambient to 315K, for Terra MODIS and Aqua MODIS. At typical blackbody temperature of 285K (for Aqua MODIS) and 290K (for Terra MODIS), the instrument response, dN_{BB} , of B21 is very small and fluctuates from scan to scan. The general scan-to-scan calibration method cannot provide accurate and stable calibration in the L1B code for band 21 because of this low-signal-to-noise ratio.

In stead of computing B21 gain on a scan by scan basis, a set of fixed linear coefficients is put into a look up table and used in L1B for the band 21 calibration. These linear coefficients are monitored and updated, if necessary, from on-orbit scheduled blackbody warm-up and cool-down cycle. Each of the 10 detectors in B21 has its own fixed coefficient. This fixed coefficient approach is specially designed for band 21, and used in both Terra and Aqua MODIS calibration.

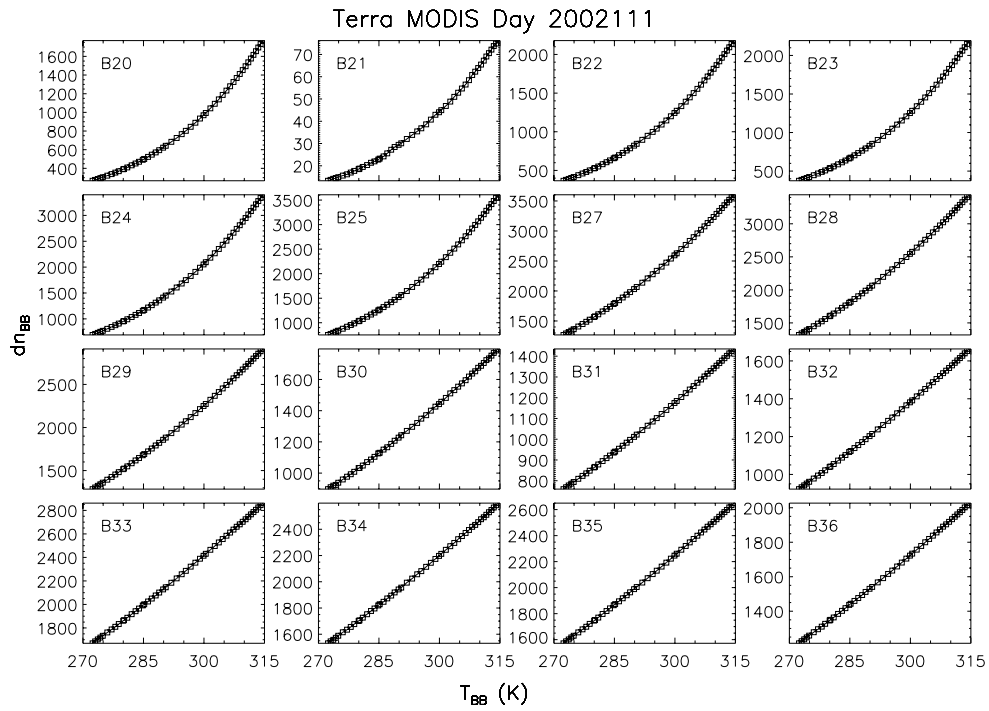


Figure 3: Terra MODIS TEB detector response to the on-board calibrator blackbody (dn_{BB}) versus blackbody temperatures (T_{BB})

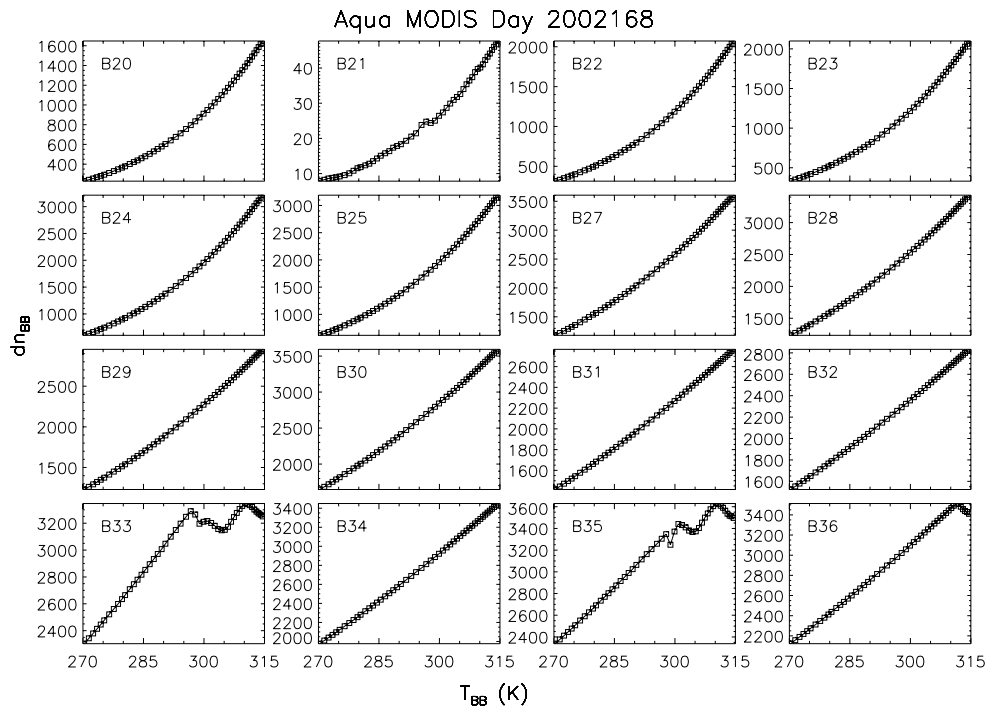


Figure 4: Aqua MODIS TEB detector response to the on-board calibrator blackbody (dn_{BB}) versus blackbody temperatures (T_{BB})

4.2 Terra MODIS PC Bands Optical Leak

Figure 5 shows the two cold focal plane assemblies (CFPAs): SMIR and LWIR. Bands 31-36 are the photoconductive (PC) bands on the LWIR FPA and the other bands are photovoltaic (PV) bands. From pre-launch instrument characterization, an optical leak from B31 to other PC bands was identified. This problem was again verified on-orbit from Earth scenes and lunar observations. Examples of Terra MODIS lunar view responses for band 31 and 33 are shown in Figure 6. The plot of band 31 (detector 5) response shows a clean and smooth profile. The response due the optical leak can be easily identified in the band 33 response profile.

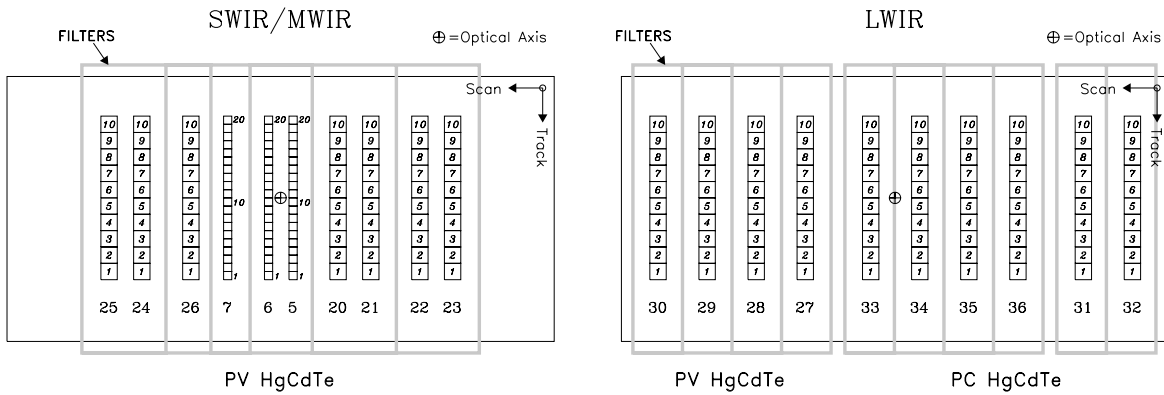


Figure 5: MODIS cold focal plane assemblies: short wave and middle wave infrared (SMIR) and long wave infrared (LWIR). Bands 31-36 are photoconductive (PC) bands and the others are photovoltaic (PV) bands

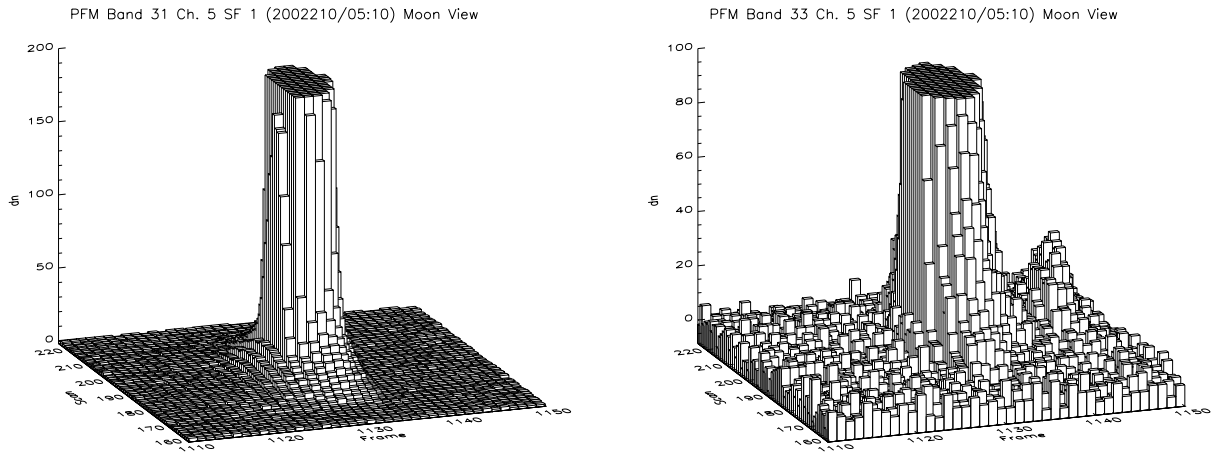


Figure 6: Terra MODIS lunar response for B31 and B33 (middle detector only). X-axis represents the data frame number, Y-axis is the scan number, and Z-axis is the response (dn). The B33 profile clearly shows the response due to the optical leak

In order to remove the optical leak from the contaminated instrument responses (dn) for these PC bands (bands 32-36), a special correction algorithm was developed and implemented in the Terra MODIS L1B code. It is designed to make the correction in the dn space by subtracting the contributions from the band 31 optical leak into the other PC bands. Assume dn^{corr} is the correct response if there were no B31 optical leak and dn^{cont} is the response with the optical leak, $xtalk_{B31 \rightarrow B}$ is the crosstalk coefficient from B31 to a given PC band, then the relationship among them (using B32 as an example) is given by,

$$dn_{B32}^{corr}(F) = dn_{B32}^{cont}(F) - xtalk_{B31 \rightarrow B32} \cdot dn_{B31}(F + FO_{B31-B32}) \quad (8)$$

where the F and FO stand for the data frame number and frame offset. The frame offset is related to band 31 and band 32 locations on the focal plane (see Figure 5). This correction is applied to B32-36 on a detector by detector basis for both the OBC BB calibration and the Earth scene (pixel by pixel) retrievals. Because of the improvements made in Aqua MODIS, there is no optical leak among the PC bands. Therefore the above correction is only used in the Terra MODIS L1B calibration algorithm.

4.3 Aqua MODIS Bands 33, 35, and 36 On-orbit Calibration

On-orbit, the BB can be operated from instrument ambient to 315K. Comparing the detector response of Aqua MODIS and Terra MODIS as a function of BB temperature as shown in Figures 3 and 4, it is noted that the Aqua MODIS bands 33, 35, and 36 saturate when the BB temperatures are above certain limits. As illustrated in Figure 2, these limits can vary due to instrument background and DC Restore (DCR). When the BB temperature is above the saturation limits, the scan by scan calibration approach of Eqn. 5 can no longer be used for these three bands.

In order to keep Earth view data calibrated in this situation, a set of LUTs that contain the calibration coefficients for B33, 35, and 36 are added and used in the L1B algorithm. These coefficients are updated, if necessary, with the most recent detector response. This approach is similar to B21 calibration. The difference is that the LUTs coefficients are only used for B33, 35, and 36 when the BB temperature is above each band's saturation limit while the LUTs coefficients are used for B21 all the time for both Terra and Aqua MODIS. This approach for calibrating B33, 35, and 36 is only required during the occasional BB warm-up and cool-down cycle calibration procedure.

5. ON-ORBIT PERFORMANCE

The Terra MODIS has been in operation for more than two and a half years. Its operational configuration was changed from the initial A-side electronics (A-I) to the B-side electronics (B) on October 30, 2000, and then switched back from B-side to A-side (A-II) using a different set of SMIR FPA biases on July 2 2001. Aqua MODIS has been in operation for less than 6 months using the B-side electronics. One of the parameters used to examine the instrument performance is the detector's noise equivalent temperature difference (NEdT). For comparison with specifications, we have listed three on-orbit measured TEB NEdT values (middle detector only) that correspond to three different configurations for Terra MODIS and one for Aqua MODIS in Table 1. Most of the detectors' NEdT values are below the specifications. All detectors of Terra MODIS B36 are out of specification since pre-launch. Aqua MODIS has made improvements in reducing the PC bands noise. Currently 9 out of 10 detectors of Aqua MODIS B36 are within the specifications. The smaller the noise, the better is the detector's short-term stability. This is shown in Figure 7 using on-orbit Terra MODIS B36 and Aqua MODIS B36 scan by scan calibration coefficients (b_1). Clearly, the performance of Aqua B36 is better due to its reduced noise.

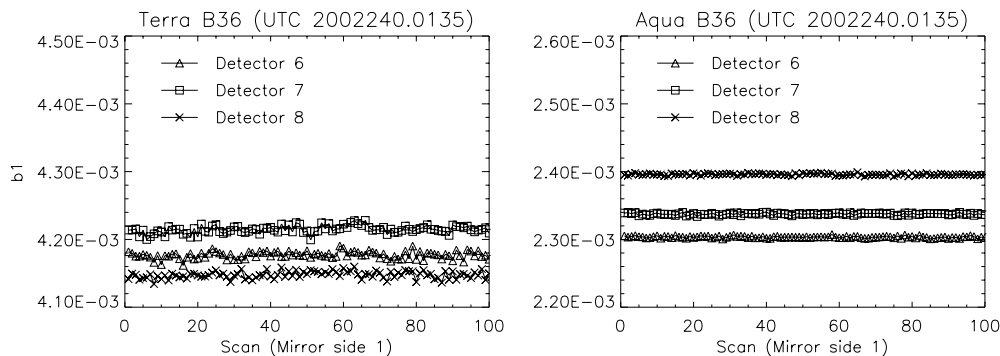


Figure 7: Terra MODIS and Aqua MODIS band 36 on-orbit calibration coefficients comparison (detectors 6, 7, and 8). Aqua B36 has much smaller scan to scan response variation. b_1 units: $W/m^2-\mu m-sr/count$

One of the modifications made in Aqua MODIS was to increase the gain of bands 31 and 32. The purpose of this was to increase the resolution of these two bands for better sea surface temperature (SST) measurements. The changes made can be seen by comparing the instrument response to the BB temperature in Figures 3 and 4. At the same BB temperature, Aqua MODIS B31 and B32 have large responses or better digital resolutions.

For Terra MODIS on-orbit calibration, an optical leak algorithm has to be used to remove the contamination from B31 to other PC bands (Equation 8). The correction coefficients were initially derived from PFM pre-launch measurements and then updated on-orbit from lunar observations and the Earth scenes⁵. Figure 8 illustrates the use and performance of our optical leak correction algorithm. The scene of these images is chosen from Baja, California. We know MODIS band 36, centered at 14.2 μ m, should not see the surface features. Because of the PC crosstalk, the surface features (brighter parts) can be seen in the Terra MODIS B36 (image 1) when no correction algorithm is applied. Image 2 shows the removal of PC crosstalk using the algorithm described earlier. The improvement is obvious. There is no optical leak in the Aqua MODIS PC bands as shown in Figure 8 image 3 for B36. No PC correction is needed for the Aqua L1B algorithm.

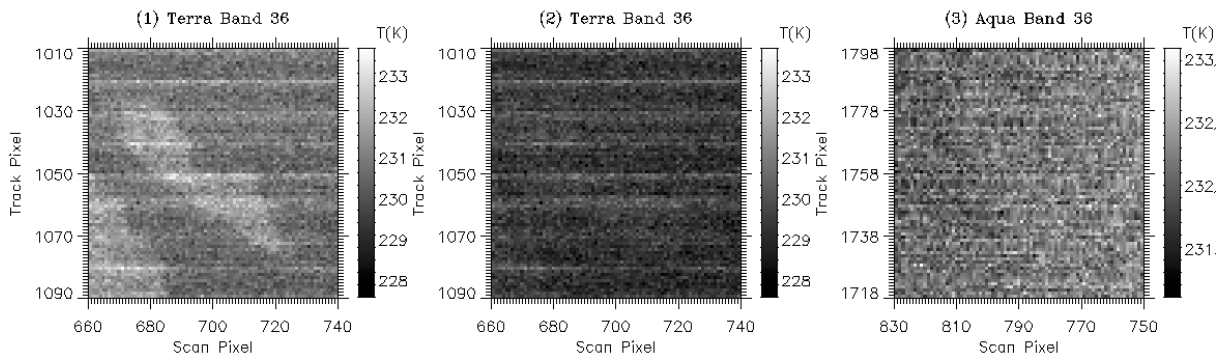


Figure 8: Terra MODIS and Aqua MODIS B36 scene images: (1) Terra B36 without correction algorithm, (2) Terra B36 with PC optical leak correction, and (3) Aqua B36 without any correction

The MODIS sensor's short-term stability, in terms of on-orbit calibration coefficients, is illustrated in Figure 9 together with several temperatures used in the calibration process. An entire orbit (100min) of data was used. The CPFAs (SMIR and LWIR) are controlled at 83K and the BB is set at 285K during this period. The scan mirror temperature is influenced heavily by the instrument temperature. One can see clearly the orbit cycling in the instrument and scan mirror temperatures from day mode to night mode. The calibration coefficients of all three detectors are very stable.

The long-term stability is demonstrated in Figure 10 using Terra MODIS over its 2.5 years of on-orbit trending of the calibration coefficients. Each selected point is a 5min (one granule of data) average. We already know from Figure 8 that the coefficient is very stable in a 5min time frame. B20 (MWIR PV band) and B31 (LWIR PC band) are used for performance evaluation. The three epochs can be clearly seen in the response trending plot: (1) day 2000055 to day 2000305 (initial A-side electronics), (2) day 2000305 to day 2000549 (B-side electronics), and (3) day 2000549 to present (A-side electronics). The gain changes in different configurations are expected. For the SMIR bands, different FPA Itwk/Vdet settings are used in the two A-side epochs. Thus the calibration coefficients (gains) are quite different. The PC bands are very sensitive to the PFA temperatures. This is shown by B31 gain changes during the period (roughly from day 2000160 to 2000216) when the CPFAs temperature could not be fully controlled due to the loss of radiative cooler margin. At a given fixed configuration with fixed FPA temperature, the TEB response is very stable. The good stability enables good quality MODIS data products.

6. SUMMARY

An overview of MODIS thermal emissive bands on-orbit calibration algorithms is given in this paper with detailed discussions on the special considerations for the low gain band calibration (B21) and for the Aqua and Terra MODIS instrument specifics. This paper also provides a number of assessments on the instrument on-orbit performance. Comparison of the detectors noise characterization has been made for both instruments under different operating conditions. Trending results from detectors response indicate good short term and long term stability. The PC optical leak correction algorithm works well on-orbit for Terra MODIS L1B algorithm. For Aqua MODIS (FM1), the improvements over Terra MODIS include better detector noise performance and the removal of the PC optical leak. Using data sets collected from both Terra and Aqua MODIS, many advanced studies can be made for better understanding of our Earth system.

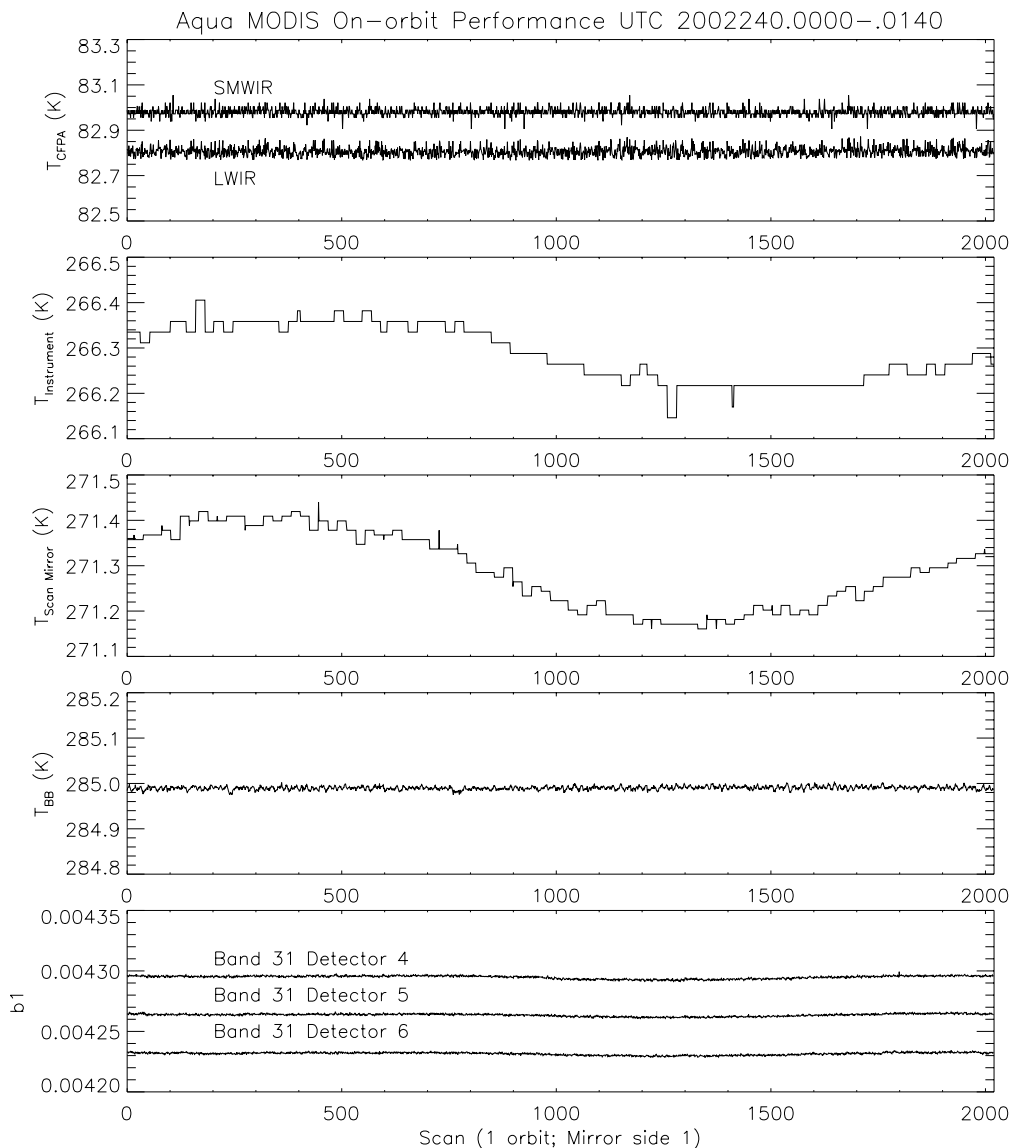


Figure 9: Aqua MODIS cold focal plane temperatures, instrument temperature, scan mirror temperature, blackbody temperature, and band 31 detectors responses (detectors 4-6, mirror side 1) over an orbit (100 minutes). b_1 units: $W/m^2-\mu m-sr/count$

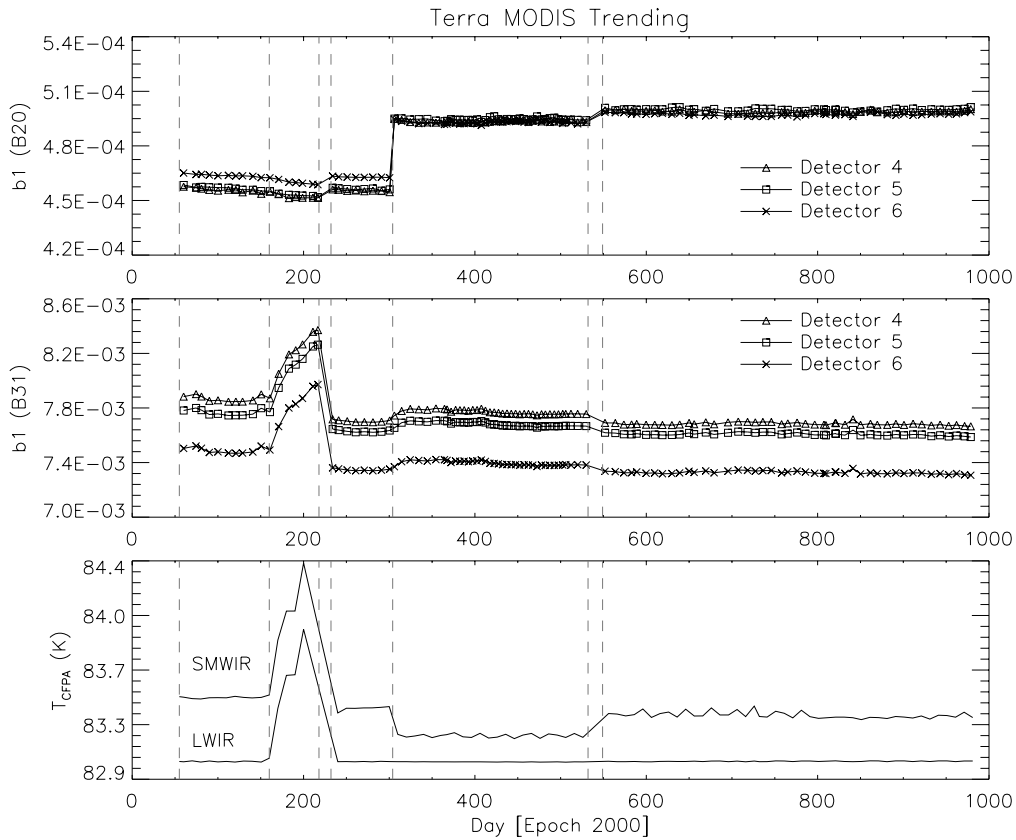


Figure 10: Terra MODIS B20 and B31 response and CFPA temperature trending over on-orbit operation days. b_1 units: $W/m^2-\mu m-sr/count$

REFERENCES

1. X. Xiong, J. Sun, J. Esposito, B. Guenther, and W. L. Barnes, MODIS Reflective Solar Bands Calibration Algorithm and On-orbit Performance , *Proceedings of SPIE — Optical Remote Sensing of the Atmosphere and Clouds III*, 4891 (2002).
2. W.L. Barnes and V. V. Salomonson, MODIS: A global image spectroradiometer for the Earth Observing System , *Critical Reviews of Optical Science and Technology*, CR47, 285-307, 1993.
3. W. L. Barnes, X. Xiong and V.V. Salomonson, Status of Terra MODIS and Aqua MODIS , *Proceedings of IGARSS*, 2002.
4. V. V. Salomonson, W. L. Barnes, X. Xiong, S. Kempler and E. Masuoka, An Overview of the Earth Observing System MODIS Instrument and Associated Data Systems Performance , *Proceedings of IGARSS*, 2002.
5. X. Xiong, J. Sun, K. Chiang, S. Xiong, and W. Barnes, MODIS On-orbit Characterization Using the Moon , *Proceedings of SPIE — Sensors, Systems, and Next Generation Satellites VI*4881 (2002).

* Xiaoxiong.Xiong.1@gssc.nasa.gov